

FORMATION, CHARACTERIZATION AND MODELLING OF THE 1987 VAL POLA ROCK-AVALANCHE DAM (ITALY)

G.B. COSTA, P. FRATTINI, N. FUSI, R. SOSIO

Dipartimento di Scienze Geologiche e Geotecnologie - Università degli Studi di Milano-Bicocca - Piazza della Scienza, 4 - 20126 Milano Italy

INTRODUCTION

Landslide dams (i.e., the natural blockage of river channels by hillslope-derived mass movements, COSTA & SCHUSTER, 1988) are natural phenomena with great relevance on geomorphological conditions and on the safety of people. Landslide dams can induce significant geomorphic hazards in the adjacent areas. Flooding by impounded water can create large lakes in the upstream areas, causing damages to human activities. Catastrophic outburst floods and/or debris flows can be triggered by a rapid dam failure with exceptional rates of sediment erosion and deposition along the downstream part of the valley.

The damming of the valley bottom can occur with different modalities (COSTA & SCHUSTER, 1988) as a function of: the landslide type (e.g. rock avalanche, debris avalanche, debris flow, rock fall, rockslide, rotational failure, rock-block slide, deep-seated complex failure, earthflow), its size and geometry, the forming material, the velocity, the size and conditions of the valley bottom, the geomorphological conditions at the landslide dam site and of the catchment upstream of the dam, the river discharge.

Fast moving and long run out landslides are among the main causes of damming because the large amount of material, rapidly transported and piled up at the valley bottom, can be eroded only through very large water discharge. Occurrence of the erosion and down-cutting of the accumulation is more difficult because of armouring by the presence of a carapace of large to very large blocks. Geometry of the valley can control the shape of the accumulation with consequences on its stability. The internal part of the accumulation is often described or assumed as homogeneous but its properties must be related to the complex motion and set of mechanisms occurring during the put in place. Translation, sliding and internal deformation or shear participate in the motion and deposition of rock avalanches as well as other granular flows.

Translation or sliding imply the resisting action at the base of the flowing material along the infinitesimal thickness of the sliding surface. The internal deformation and the interaction with a rough basal topographic surface imply the resisting action of the flowing material along its entire thickness under variable stresses. Entrainment or deposition of the material can induce important changes in momentum, volume, material properties, and runout distance. This complexity is at the origin of many different theories proposed to explain

the exceptional mobility of rock and debris avalanches.

We present and discuss data from the 1987 Val Pola rock avalanche. Field surveys, in situ and laboratory tests are presented and discussed as means to perform modeling of the landslide movement and of the evolution of the accumulation.

THE VAL POLA ROCK AVALANCHE

On July 1987, the central Alps experienced a period of exceptionally rainfall with the 0°C isotherm positioned at very high elevations. 600-mm of rain, half of the mean annual precipitation for the Valtellina area (central Italian Alps), fell between 15th and 22nd July 1987 (COSTA, 1991; COSTA, 1991; COSTA *et alii*, 2004) causing flooding and hundreds of landslides.

The Val Pola landslide, occurred in the upper Valtellina on the slope of Mount Zandila. The upper sector of this slope was part of a large prehistoric landslide located at the intersection of two major joint sets. Bedrock consists of tight northward-dipping isoclinal folded and highly fractured and tectonized diorite and gabbro (Gabbro di Sondalo), ortho-quartzite and amphibolite (Mte Tonale Formation) and fine-grained gneiss (Val Grosina Formation). The prehistoric landslide, identified by a 700 m long and 100 m high head scarp, was located between 1650 m a.s.l. and 2350 m a.s.l.

On 18-19 July 1987 intense and continuous rainfall caused flooding and numerous superficial rockfalls and debris flows along the Val Pola creek, at the northern margin of the landslide. Debris flows formed a large alluvial fan that dammed the Adda River valley and caused the formation of a 50000 m³ lake up to 5 m deep.

On July 25, a 600 m long fracture developed at the base of the old head scarp, and reached 900m on July 28 when at 7:23 am, about 50 millions of cubic meters of rock detached from the slope, moving downslope up to the valley bottom, raising for 300 m on the opposite valley flank and flowing both upstream (up to 2.7 km as a mud wave) and downstream (up to 1.5 km, Figure 1) along the valley. The estimated maximum runout velocity of the avalanche ranged from 76 m s⁻¹ up to 108 m s⁻¹, based on potential energy conversion (COSTA, 1991; COSTA, 1991) and from 50 m s⁻¹ to 75 m s⁻¹, based on numerical modelling (COSTA *et alii*, 2003; 2004). The landslide destroyed 3 villages and claimed 27 lives.

GEOMORPHOLOGIC FEATURES OF THE ACCUMULATION

The avalanche deposits were poorly sorted, consisting of angular coarse blocks, up to several meters in diameter, and fine rock debris. Ridges and furrows, largely parallel to the valley axis (Figure 1), secondary slides, scarps, poorly sorted hummocky surfaces, and flow-like features were observed within the accumulation. Fine-grained materials were concentrated on the lee-side. Alluvial and lacustrine sediments, scoured by the moving mass from the valley bottom, were found at various sites. Coarse blocks, up to few mega blocks, and gravel prevailed at the surface and toe of the slope, and at the down-slope tip of the deposit. Inverse grading was not evident apart in the uppermost and outermost sectors.

61 samples, 6 kg to 20000 kg in size, were collected at the surface or just below it in the deposition area, 4 samples were collected within the source area, 109 samples were collected by means of 21 boreholes.

Blocks and gravel at the deposit surface (Figure 2a) range from 8 to 95%, sand from 10 to 75 %, and silt and clay from 6 to 60%. Blocks almost completely form 10 of the 61 superficial samples. Silts are usually less than 10%. Fine matrix (< 0.075 mm) forms in a few cases 50 to 95 % of the samples. The coefficient of uniformity ($U=D_{60}/D_{10}$; Figure 2b) is usually low. Samples taken from within the bowl-shaped source area are well graded with a low degree of sorting. Gravel ranges between 30 to 60%, sand between 40 to 70% and finer than 0.075 mm are usually less than 5%. Blocks and pebbles are present as in the main deposit. On the basis of direct measurements and image analysis of photos of the deposits, fragments were prevalently angular and sub-angular, equant-spherical and oblate-disk shaped with no dependence on size, location and depth. Larger elements showed a jigsaw fabric.

We observed (Figure 2b and 3) a slight decrease in average grain size with depth and an increasing value of the uniformity coefficient, U , and then the presence of well graded materials within the deposit (Figure 3).

Blocks within the deposit range from few percents to 40% and are generally more abundant close to the surface, at the toe of the failed slope and at the extreme terminal tips of the deposit. Gravel follows a similar trend within the initial 30 m with a progressive increase in the sandy grain size fraction. Silt and clay remains below 10% up to 30 m, to increase up to about 37% between 30 and 70 m. We associate this increase in finer material with the entrapment of alluvial material or the sampling below the base of the accumulation. 7 more samples were collected from trial pits for bulk weight (19.8-21.6 kN/m³) and specific gravity (2.75-2.88) evaluations and large-scale triaxial tests (at confining pressures: 0.1-0.6 MPa, samples with a 100 mm maximum grain size, 500 mm in diameter and 1,000 mm in height; bulk weight between 21.0 and 22.5 kN/m³; porosity of 20-24.5 %; internal friction angle: 45°-47° with no cohesion).

Permeability of the deposit was evaluated at different sites with

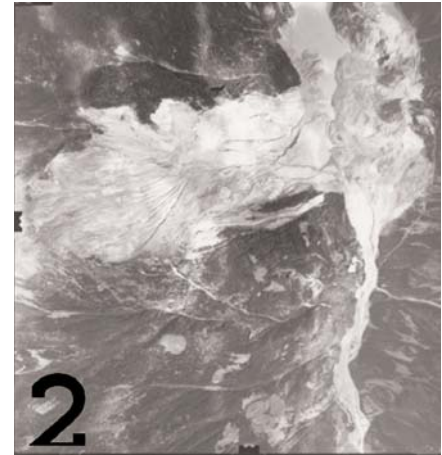
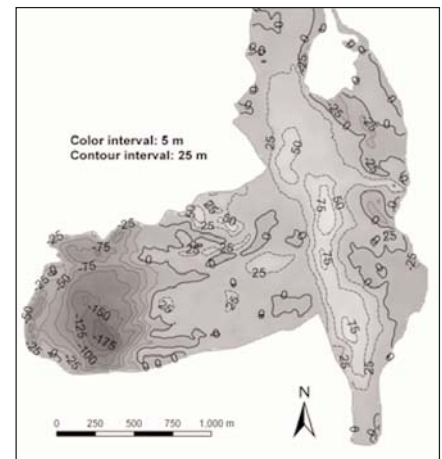


Figure 1
a) Aerial photo of the Val Pola rock avalanche area just after the overtopping of the landslide

b) Map of the changes in elevation dam



different techniques: pit infiltrometric tests (1.2×10^{-4} - 1.1×10^{-3} m s⁻¹), variable head tests within boreholes and tracer tests (2.7×10^{-3} m s⁻¹). Hydraulic conductivity values ranges between 10^{-6} and 10^{-2} m s⁻¹ with a dispersion of about two orders of magnitude at similar depths.

We observe a progressive decrease of hydraulic conductivity with depth, from 10^{-5} m s⁻¹, close to the surface, up to 10^{-6} m s⁻¹, at 70 m.

Geophysical surveys by the superficial shear waves (SSW) technique identified three main layers between 0 and 4 m, with shear wave velocity, V_s , between 200 and 300 m s⁻¹; between 4 and 15 m, with $V_s = 600$ -1000 m s⁻¹; and below 15 m with $V_s = 1700$ m s⁻¹.

HYDROGEOLOGICAL DATA

The stability of landslide dams is controlled by mechanical and hydrogeologic characteristics. The Val Pola case study allowed, beyond the physical parametrization of the accumulation, the observation of water level rising and perturbation of the flow conditions during the rise of the lake level. This has been accomplished by means of 21 piezometers drilled within the accumulation and monitored during lake level rising, pumping and dam overtopping. The catchment area at the landslide dam site was 533 km² and included

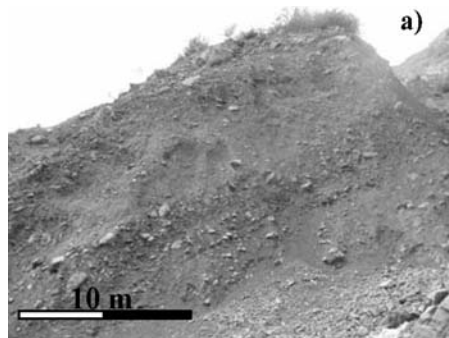
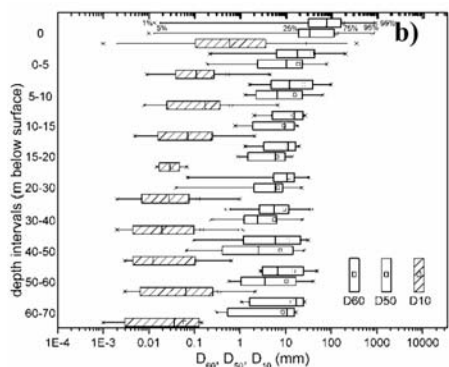


Figure 2
a) Rock avalanche deposits at the toe of the slope with evidences of discontinuous and irregular layering, together with inverse gradation in the upper part



b) box and whiskers plot showing the trend with depth for the characteristic diameters (D10, D50, D60)

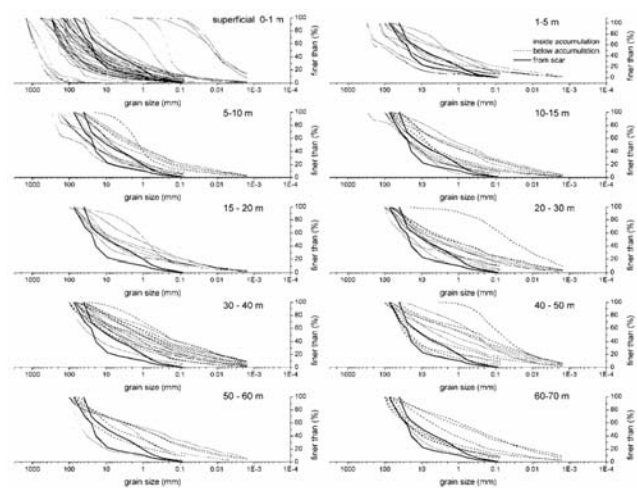


Figure 3 - Grain size curve for 174 samples collected at different sites and depths within the accumulation. Samples are plotted in groups for different depth intervals. Grain size curves interval for samples from the landslide source scar is shown with two thick lines on each plot

two artificial lakes. Between July 28th and August 23rd the lake level raised about 0.5 m d⁻¹ up to 1089.65 m a.s.l. for a total area of 570000 m². On August 24th-25th the water level reached 1097.62 m a.s.l. (761000 m²) after a 200 mm rainfall. Between August 27th and 30, a 2 km long rip-rapped spillway channel, was excavated at 1102 m a.s.l. and the downstream slope of the landslide dam was levelled

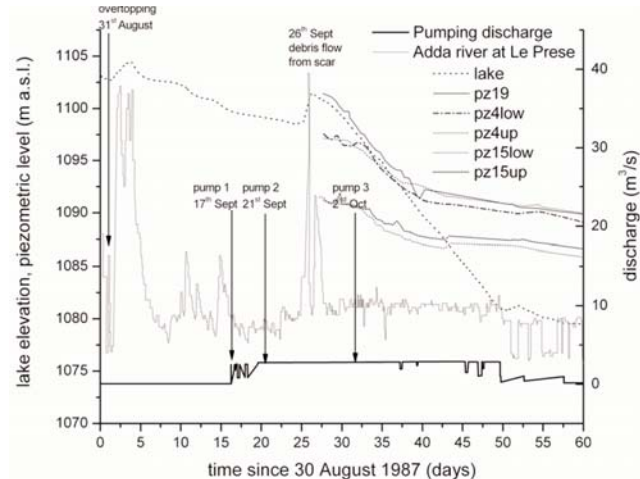


Figure 4 - Lake level and piezometric levels, measured in some of the 21 piezometers, since August 30, 1987. Discharge of the Adda river as measured at Le Prese and of the pumping system are also represented

to reach an 8 to 12% average slope. Overtopping started on August 29th, with a 35 m³ s⁻¹ water discharge at the inlet of the channel and an impounded lake of 22x10⁶ m³, after 25000 people were evacuated from the downstream area. No outflow was observed. On August 31st water started to flow on the entire length of the channel (Figure 4). A water pumping system started working on September 17th with a maximum discharge of 6 m³ s⁻¹. Overtopping caused the erosion of the downstream slope of the dam with erosion and subsequent deposition of a large amount of debris just downstream. On September 26th a peak discharge was caused by a large debris flow which dammed the spillway channel inducing a rapid increase in the lake level.

Monitoring showed that the piezometric level (Figure 4) reacted immediately to lake level changes close to the lake itself and only after ten days on the downstream side of the accumulation.

DAM BREAK FLOOD ASSESSMENT

Failure of natural dams, by overtopping, piping or general failure, represent a relevant hazard to people and property. Overtopping is the failure mechanism most frequently observed for natural dams. Most of the observed failures usually occur within the first year since the landslide dam formation (Figure 5).

An initial emergency assessment of the peak discharge (16500 m³ s⁻¹) has been done by Costa relationship (COSTA, 1991) for the Val Pola landslide dam. We re-examine this subject by using all the collected data and considering the approaches made available since 1987. We use empirical regression relationships, parametric methods, dimensionless analysis and physically based models. The volume of the lake, the height of the dam or the depth of the lake, the breach width and its development time are the most important controlling factors.

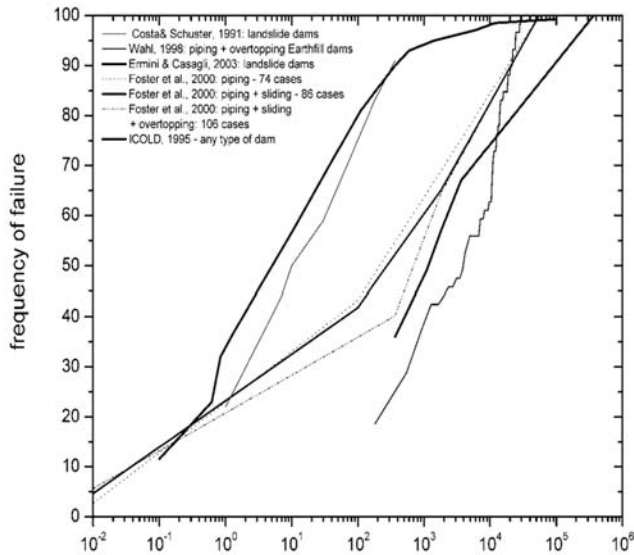


Figure 5 - Frequency of failure for different times after formation/construction for different types of dams: natural and artificial, as consequence of different mechanisms of failure (piping, overtopping, sliding) and according to different authors

Empirical relationships, in the form of regression or envelope curves, are a rapid method of determining the order of magnitude of peak discharge, but they are characterised by a high degree of uncertainty. Using some of the empirical regressions and envelope relationships, proposed in the literature (see Table I), we obtained values of peak discharge ranging between $2492 \text{ m}^3 \text{ s}^{-1}$ and $4487 \text{ m}^3 \text{ s}^{-1}$, and between $97341 \text{ m}^3 \text{ s}^{-1}$ and $133946 \text{ m}^3 \text{ s}^{-1}$, respectively.

Table I shows also the mean values and the computed standard deviations which give evidence of the dispersion of the values. We computed the breach size (mean width ca. 161.5 m; basal width. 100-118 m; top width: 204-222 m) and the breach failure time ($t_f = 46 \text{ min}$ ca.) through Froehlich's relationship (FROEHLICH, 1995). The approaches proposed by FREAD (1984; 1988) and WETMORE & FREAD (1991) (SMPDBK) were used for the determination of the peak discharge by taking into account the computed breach dimension and the failure time. The peak discharge values ranged between $2360 \text{ m}^3 \text{ s}^{-1}$ and $19731 \text{ m}^3 \text{ s}^{-1}$. Available data have been used to compute the instantaneous peak discharge through adoption of broad-crested weir equations resulting in values ranging between 2570 and $3310 \text{ m}^3 \text{ s}^{-1}$. Monte Carlo analyses performed by means of different models with different values for the main variables (e.g. dam height, final breach width, elevation of breach base) allow to evaluate the probability of occurrence for a certain value of peak discharge. We observe the variability of the results due both to the type of approach (FREAD, 1984, 1988; Figure 7; WETMORE & FREAD, 1991; COLEMAN *et alii*, 2002) and to their sensitivity to the change in value of the controlling variables, and uncertainty in parameter assessment. We analyse the sensitivity of the models due to the difficulty in defining both the geometry of the landslide dam (irregular geometry controlled by the pre-

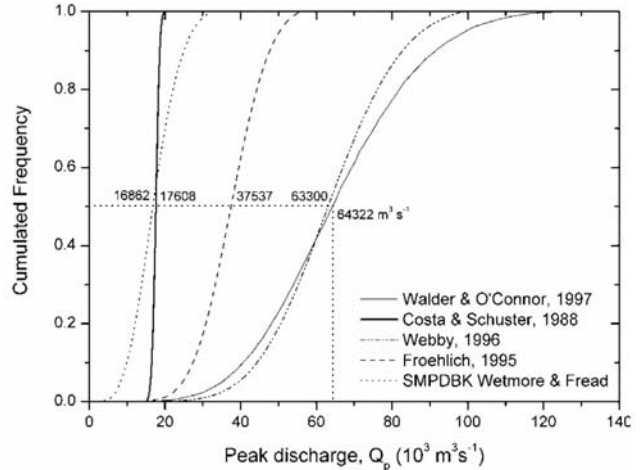


Figure 6 - Plot of the results of Monte Carlo simulations (10000 runs, Latin-Hypercube sampling) performed for different approaches. Range for each variable: dam height: 30 - 90 m; breach height: 15-55 m; mean breach width: 50 - 221 m; lake area: 1.42 km²; lake volume: $22 \cdot 10^6 \text{ m}^3$

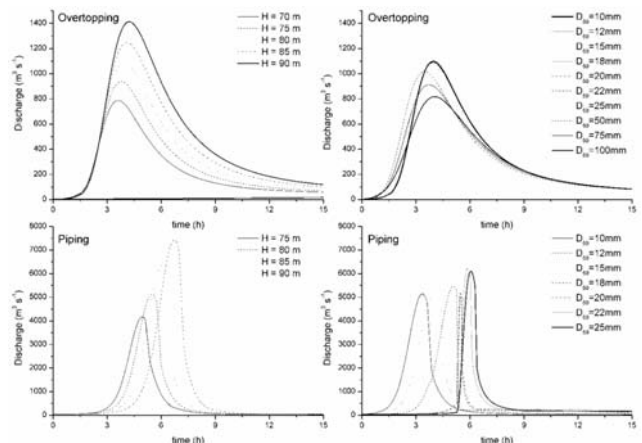


Figure 7 - Sensitivity of BREACH model for overtopping and piping failure to changes in values of D50 (right) and to dam height (left). Origin of the plots (time 0) has been put at a fixed discharge value ($40 \text{ m}^3 \text{ s}^{-1}$)

existing morphology of the valley, along longitudinal and transversal profiles, downstream sloping valley profile, the geometric features of the accumulation) and the representative grain size.

DISCUSSION AND CONCLUSIONS

We observed that the material forming the Val Pola landslide deposits was relatively coarse but was also fining downward and well graded and that it is common to pass from a grain supported texture to a matrix supported one by simply moving vertically within the accumulation or approaching the surface. We rise some major questions concerning the data usually collected and used to present some

FORMATION, CHARACTERIZATION AND MODELLING OF THE 1987 VAL POLA ROCK-AVALANCHE DAM (ITALY)

| Reference | Eq. | Q_p $m^3 s^{-1}$ | Mean $m^3 s^{-1}$ | St. Dev. $m^3 s^{-1}$ |
|-------------------------|--------------------------------------|-----------------------|----------------------|--------------------------|
| Regression equations | | | | |
| Costa, 1985 | $Q_p = 672 \cdot (V_o/10^6)^{0.56}$ | 3794 | | |
| | $Q_p = 6.3 \cdot d^{1.39}$ | 2492 | | |
| | $Q_p = 181 \cdot (dV_o/10^6)^{0.43}$ | 3446 | | |
| Costa & Schuster, 1988 | $Q_p = 0.0158 \cdot E_p^{0.41}$ | 3276 | | |
| Walder & O'Connor, 1997 | $Q_p = 1.6 \cdot V_o^{0.46}$ | 3816 | | |
| | $Q_p = 6.7 \cdot d^{1.73}$ | 4487 | | |
| | $Q_p = 0.99 \cdot dV_o^{0.40}$ | 3855 | 3595 | 618 |
| Envelope equations | | | | |
| Costa & Schuster, 1988 | $Q_p = 0.063 \cdot E_p^{0.42}$ | 17608 | | |
| Walder & O'Connor, 1997 | $Q_p = 46 \cdot V_o^{0.46}$ | 109717 | | |
| | $Q_p = 200 \cdot d^{1.73}$ | 133946 | | |
| | $Q_p = 25 \cdot dV_o^{0.40}$ | 97341 | 89653 | 50379 |

Table I - Results obtained by application of the empirical relationships proposed in the literature by different authors both for artificial and landslide dams. V_o : volume of water released (complete failure: $22 \times 10^6 m^3$); d : lake depth (max depth: 43 m); E_p : potential energy of stored water ($\rho_w \cdot g \cdot d \cdot V_o$)

assumptions about mechanisms of movement and deposition.

Grain size analyses show a certain homogeneity of the landslide accumulation with two major sectors: the carapace, or the coarse sorted superficial zone, and the finer inner well graded part which forms most of the mass. The existence of a thin basal low density and high particle velocity basal shear layer is frequently assumed when modeling granular avalanches down steep incline. This behaviour has been observed in laboratory tests and numerical models on monosized materials, under low stress levels, with no particle breakage, in motion along very smooth and regular surfaces. These conditions seem quite different from those characteristic of very large rock- and debris-avalanches. Phenomena observed in nature are generally characterised by: breakable particles, very irregular superficial morphologies, extremely high stress levels. As a consequence we can infer that many particular and local conditions can control both external and internal structures of the landslide accumulation, and that local or point-like descriptions are not sufficient to give a complete idea of the problem.

Our observations also suggest that the difference in grain size between debris forming the accumulation or present in large quantities within the bowl shaped scarp of the Val Pola rock avalanche are quite small. This contrasts with the assumption that the material

undergoes a strong decrease in grain size during its motion along the slope. The change in grain size seems less important than usually assumed and could exclude the feasibility of some particular mechanisms or minimize their relevance in controlling landslide mobility. Numerical models of the transportation and runout phases of a rock avalanche (CROSTA *et alii*, 2003, 2004) have also shown that different material behaviours can involve completely different strain distributions within the moving mass. As a consequence a different degree of shearing and grinding can be experienced by the material within the moving mass according to its behaviour.

Rock- and debris-avalanches are usually characterized by long runout and peculiar mechanisms of transport and deposition typical of many granular movements. Grinding, shearing, fragmentation, segregation, soil, water and ice entrapment, can occur in these instabilities.

Texture controls the stability of the landslide dams, by influencing the geotechnical and hydrogeological properties of the dam material. Dams showing a higher degree of stability, with no catastrophic failure, are those characterised by coarse grain sizes and grain-supported textures. Rock and debris-avalanche deposits show vertical and lateral changes in grain size. Parts of the deposits can work sometimes as a filter to respect to other sectors.

Finally, we have shown, by a Monte Carlo approach, how the uncertainty in the definition of representative values for the controlling parameters (e.g. mean particle size, dam height, gradient of the base of the dam, length and width) can strongly influence the computed values of the peak discharge and the flood duration.

ACKNOWLEDGEMENTS

The research has been funded by the EC Project LessLoss - N.: GOCE-CT-2003-505448 – EC and by the Ministry of Education: Catastrophic slope failures: Characterization, monitoring and modelling for hazard assessment PRIN 2003-MIUR, and Multidisciplinary approach for large landslide hazard assessment FIRB 2001-MIUR. The Regione Lombardia and Ismes-CESI are thanked for making data available.

REFERENCES

COLEMAN S.E., ANDREWS D.P. & WEBBY M.G. (2002) - *Overtopping breaching of noncohesive homogeneous embankments*. Journal of Hydraulic Engineering, 128, 9: 829-838.

COSTA J.E. (1985) - *Floods from Dam Failures*. U.S. Geol. Surv. Open File Rep. 85-560, Denver, Colorado, 54 pp.

COSTA J.E. (1991) - *Nature, mechanics, and mitigation of the Val Pola landslide, Valtellina, Italy, 1987-1988*. Zeitschrift für Geomorphologie, 35: 15-38.

COSTA J.E. & SCHUSTER R.L. (1988) - *The formation and failure of natural dams*. Geological Society of America Bulletin, 100: 1054-1068.

COSTA J. E. & SCHUSTER R. L. (1991) - *Documented historical landslide dams from around the world*. U.S. Geol. Surv. Open File Rep. 91-239: 486 pp.

CROSTA G. (1991) - *Studio di movimenti in massa. Modellizzazione teorica e sperimentale con osservazioni e rilievi di campagna*. PhD Thesis, Univ. Studi di Milano, 137 pp.

CROSTA G.B., IMPOSIMATO S. & RODDEMAN D.G. (2003) - *Numerical modelling of large landslides stability and runout*. Natural Hazards and Earth System Sciences, 3 (6): 523-538.

CROSTA G.B., CHEN H. & LEE C.F. (2004) - *Replay of the 1987 Val Pola Landslide, Italian Alps*. Geomorphology, 60 (1-2): 127-146.

- ERMINI L. & CASAGLI N. (2003) - *Prediction of the behaviour of landslide dams using a geomorphological dimensionless index*. Earth Surf. Process. Landforms, **28**: 31–47.
- FOSTER M. A., FELL R. & SPANNANGLE M. (2000) - *The statistics of embankment dam failures and accidents*. Can. Geotech. J., **37** (5): 1000–1024.
- FREAD D.L. (1984) - *DAMBRK: The NWS Dam-Break Flood Forecasting Model*. National Weather Service, Office of Hydrology, Silver Spring, Maryland.
- FREAD D.L. (1988) - *BREACH: An Erosion Model for Earthen Dam Failures*. National Weather Service, National Oceanic and Atmospheric Administration, Silver Spring, Maryland, 35.
- FROELICH D.C. (1995) - *Peak Outflow from Breached Embankment Dam*. Journal of WaterResources Planning and Management, **121** (1): 90-97.
- ICOLD (1995) - *Dam failures — statistical analysis*. Bulletin 99 of the International Committee on Large Dams (ICOLD), Paris, France, ISSN 0534-8293, 73 pp.
- WAHL T.L.(1998) - *Prediction of embankment dam breach parameters, a literature review and needs assessment*. Rep. No. DSO-98-004, Bureau of Reclamation, U.S. Dep.of the Interior, Denver, 67 pp.
- WALDER J.S. & O'CONNOR J.E. (1997) - *Methods for Predicting Peak Discharge of Floods Caused by Failure of Natural and Constructed Earth Dams*. Water Resources Research, **33**, 10: 2337–2348.
- WETMORE J.N. & FREAD D.L. (1991) - *The NWS Simplified Dam Break Flood Forecasting Model*. Federal Emergency Management Agency (FEMA). 36pp.